Physicomechanical Studies and Solvent Resistance Analysis of Melt-Blended Novel Ethylene-1-Octene Elastomer and Ethylene-*co*-Acrylic Acid Interpenetrating Network Hybrids

Baisali Gupta,[1] Deepanjan Banerjee,[1] Luna Goswami,[2] Abhijit Bandyopadhyay[2]

[1]*Application Research and Development Centre, Haldia Petrochemicals, Limited, 54/A/1, Block DN, Sector V, Saltlake City, Calcutta 700091, India*
[2]*Department of Polymer Science and Technology, University of Calcutta, 92, Acharyya Prafulla Chandra Road, Calcutta 700009, India*

Received 20 October 2009; accepted 29 August 2010
DOI 10.1002/app.33345
Published online 14 February 2011 in Wiley Online Library (wileyonlinelibrary.com).

ABSTRACT: Polar modification of poly(ethylene-*co*-octene) (POE) elastomer was carried out with a relatively new approach. Poly(ethylene-*co*-acrylic acid) (EAA) was taken as the modifier and POE with a calculated amount of EAA were coextruded with dicumyl peroxide (DCP; used as a crosslinker). The majority of the compositions showed the existence of a crosslinked EAA phase inside POE, although increasing DCP concentrations and extrusion temperatures were possibly capable of crosslinking either of the phases, as observed with a model composition. All of the samples were soft and light in nature. The best composition was the one that contained 13.3 wt % EAA; that composition showed excellent surface polarity and superior mechanical properties. Detailed solvent swelling experiments also yielded the best results for that particular composition. © 2011 Wiley Periodicals, Inc. J Appl Polym Sci 120: 3401–3409, 2011

Key words: blending; crosslinking; elastomers; modification

INTRODUCTION

Polyolefin elastomers are a new class of polymers with great potential for wide industrial application.[1] The metallocene catalyst selectively polymerizes ethylene and comonomer sequences and enhances the elasticity of the resulting materials as comonomer incorporation disrupts the polyethylene crystallinity.[2] Furthermore, the molecular weight of the copolymer helps to determine its processing characteristics and end-use performance, with higher molecular weights generally providing enhanced toughness. The most popular polyolefin elastomers are manufactured by Dow-DuPont under the trade name ENGAGE.[3] The two most popular grades of polyolefin elastomers are poly(ethylene-*co*-octene) (POE) and poly(ethylene-*co*-butene) with various comonomer contents and overall crystallinities. In this study, we selected high-crystallinity-grade POE as the base elastomer for detailed investigation because of its low melting temperature and easy processing characteristics. POE has several other advantages, including easy handling, better compound economy because of its reduced modifier levels, reduced weight via lower density products, and narrow molecular weight distribution.[4] These are excellent materials for impact modification in hydrocarbon polymers such as polypropylene[5,6] and in polar polymers such as nylons.[7] The principal drawbacks, as a whole, for polyolefin elastomers include poor surface properties, poor affinity toward polar polymers and fillers, and inferior solvent resistance, especially in hydrocarbon solvents. These have been assigned primarily because of the purely nonpolar structure of the elastomer. Some recent studies of polyolefin elastomers have been undertaken to modify these elastomers to impart polarity and to overcome these limitations. The grafting of small molecules such as maleic anhydride[8] and acrylic acid (AA)[9–11] onto polyolefin elastomers have been successfully tried and have been reported in the literature. The reactions have been performed both in the melt and in solution stages. Reports on the use of grafted POE as a toughening agent in polymers are also available. For example, González et al.[12] reported the characteristics of the brittle/tough transition of poly(butylene terephthalate)/maleinized POE blends by using an

Correspondence to: A. Bandyopadhyay (abpoly@caluniv.ac.in).

Contract grant sponsor: Science and Engineering Research Council Division, Department of Science and Technology, Government of India under Fast Track Scheme for Young Scientists (to A.B.); contract grant number: SR/FTP/ETA-23-08.

essential work of fracture procedure. Arostegui and coworkers[13,14] performed the synthesis of supertoughened poly-(butylene terephthalate) using phenoxy and maleic anhydride grafted POE. The grafting of other agents such as silanes onto POE was reported by Jiao et al.[15] He et al.[16] reported the grafting of undecyclenic acid onto POE. Peroxides such as benzoyl peroxide are normally used as the grafting initiator in most of these cases, and the crosslinking of POE cannot be avoided as a major side reaction in these processes. In fact, graft and gel formations have been found to go parallel with each other.[9]

In this study, we tried to modify POE by a relatively new approach. POE was melt-blended with a polar ethylenic copolymer such as poly(ethylene-*co*-acrylic acid) (EAA), and we also attempted *in situ* networking using dicumyl peroxide (DCP). EAA was selected as the modifier for POE in this study primarily because of the similarity in their polyethylenic backbone structures [POE solubility parameter (δ) = 16.68 $J^{1/2}$ $cm^{-3/2}$ and EAA δ = 18.30 $J^{1/2}$ $cm^{-3/2}$], which gave the possibility of rendering good technical compatibility and resistance to macrophase separation at the initial stage of mixing. The mixing was done in a single-screw extruder through a multipass technique. The different process variables were the EAA and DCP concentrations and extrusion temperature. The resulting blend morphologies were investigated through combined studies on the gel content and Fourier transform infrared (FTIR) spectroscopic analysis. The samples were further characterized through surface energy measurements and mechanical properties analysis. The solvent resistance properties were analyzed in detail through the selection of a series of polar and nonpolar solvents having close proximity in their δ's with POE and EAA.

EXPERIMENTAL

Materials

POE elastomer (ENGAGE 8440, comonomer content = 23 wt %, density = 0.897 at 25°C, total crystallinity = 27%, and glass transition temperature = −44°C) was procured from Dow Chemicals (Taloja, Maharashtra, India). It was reported to have a melt flow index of 1.6 dg/min (ASTM D 1238, 190°C, 2.16 kg). In this article, this is referred to as POE. EAA (ESCOR 5200) was an ethylene–AA copolymer with a high comonomer content (15 wt %) and was obtained from Exxon Mobil Chemical (Harbour Front Place, Singapore). It had a melt flow index (ASTM D 1238) of 38 g/10 min and a density of 0.944 at 25°C. This is referred to as EAA in this article. DCP (98% pure grade) was procured from Aldrich Chemicals (Kolkata, India). The solvents, xylene (δ = 18.2), ethyl acetate (δ = 18.2), tetrahydrofuran (THF; δ = 18.5), diethyl ether (δ = 15.4), dimethylformamide (DMF; δ = 24.7), and hexane (δ = 14.9), all laboratory grade, were obtained from indigenous sources and were used as received.

Sample preparation and sample composition

POE was mixed and extruded with variable weight proportions of EAA and DCP (wt %) with a single-screw extruder (length/diameter ratio = 20/1, S. C. Dey and Co., Kolkata, India) at different temperatures. A uniform screw speed of 60 rpm was maintained for all of the compositions. The samples were re-passed three times through the extruder to ensure proper phase mixing, and the data reported on processing parameters are the numerical average of three values. The concentration of EAA in the blends was adjusted to give a net AA content of 0–15 wt % in the hybrid samples. The extrudates were quenched in a tank containing water at 20–30°C and then pelletized. The pellets were compression-molded at 180°C for 4 min under 25 MPa of compressive pressure in a 30-ton capacity compression-molding machine (S. C. Dey and Co., S-1112). Details of the blend compositions, their specific gravities, and Shore D hardness values are reported in Table I.

Characterization

Determination of the free energy of mixing (ΔG_{mix}) and Flory–Huggins interaction parameter (χ) for the POE–EAA blends

ΔG_{mix} and χ were calculated with eq. (1):

$$\Delta G_{mix} = RT[(1/V_1)\varphi_1(\ln \varphi_1)] + [(1/V_2)\varphi_2(\ln \varphi_2)] + \chi\varphi_1\varphi_2 \quad (1)$$

where R is universal gas constant, T is temperature in absolute scale and ΔG_{mix} is the free energy per unit volume of the mixture; V_1 and V_2 are the molar volumes of polymers 1 and 2, respectively; and φ_1 and φ_2 are the volume fractions of polymers 1 and 2, respectively.

V_1 and V_2 in eq. (1) were calculated from the structural contributions of POE and EAA. φ_1 and φ_2 were calculated from the weight percentage compositions of the samples.

Measurement of the die swell and extrusion time

Extrudates emerging from the die of the extruder were collected for die swell measurements [eq. (2)], and maximum care taken to prevent any further deformations:

$$\text{Die swell ratio} = (\text{Diameter of the extrudate}/\text{Diameter of the die}) \quad (2)$$

The extrusion time was taken as the time from feeding the mass (100 g per batch) until that came

TABLE I
Compositions of the Samples

Sample designation	POE content (phr)	EAA content (phr)	AA (phr)	DCP (phr)	Die temperature (°C)	Specific gravity	Hardness (Shore D)
R	100	0.0	0.0	0.2	200	0.897	28
$R_{.5}$	100	3.3	0.5	0.2	200	1.07	28
R_1	100	6.7	1.0	0.2	200	1.07	30
R_2	100	13.3	2.0	0.2	200	1.02	28
R_5	100	33.3	5.0	0.2	200	1.02	30
R_7	100	46.7	7.0	0.2	200	1.02	30
R_{10}	100	66.6	10.0	0.2	200	1.06	28
R_{15}	100	100.0	15.0	0.2	200	1.06	28
$R_{2P.4}$	100	13.3	2.0	0.4	200	1.04	28
$R_{2P.6}$	100	13.3	2.0	0.6	200	1.05	30
R_{2T215}	100	13.3	2.0	0.2	215	1.04	28
T_{2T230}	100	13.3	2.0	0.2	230	1.04	28
A	0	100.0	15.0	0.2	200	0.94	26

out from the extruder and was recorded manually for each experiment.

FTIR spectroscopic analysis

FTIR spectroscopic analysis of all of the samples was made with a Jasco FTIR machine (Jasco International Company Ltd., Hachioji, Tokyo, Japan) within the spectral range 400–4000 cm^{-1} with a resolution of 4 cm^{-1} in dispersive mode. An average of 120 scans for each sample was reported for the analysis.

Determination of the gel content by the solvent extraction method

The gel content of all of the extrudate samples were measured by extraction with a 50–50 (wt %) mixture of hot xylene and DMF in a Soxhlet apparatus (Loba Chem, Mumbai, India) for 24 h. The undissolved portion of the samples was assigned as the gel. The gels were air-dried to a constant weight to remove the associated solvents, and the final weight was taken to calculate the gel percentage for each composition [eq. (3)]:

$$\%\,\text{Gel} = (\text{Weight of the remnant sample})/(\text{Initial weight of the sample}) \times 100 \quad (3)$$

Measurement of the contact angle (θ) and work of adhesion (W)

The postmodification surface characteristics of POE were determined with a θ meter (Thermo Cahn Radian 300) with formamide as the probe liquid. The equilibrium values were obtained in 15 min, and hence, all of the experiments were performed up to 15 min. Each θ reported is the mean of six measurements with a maximum error in θ of ±1°. All investigations were carried out with a polymer plate with dimensions of $10 \times 10 \times 2$ mm^3 in vapor-saturated air at 20 ± 2°C in a closed sample box after careful cleaning of the surface with ethanol and further examination of gross undulations under an optical microscope. W was calculated from θ data with eq. (4):

$$W = Y_1(1 + \cos\theta) \quad (4)$$

where Y_1 is the surface energy of the formamide (58 mJ/m).

Studies of the mechanical properties

The tensile strength and elongation at break were measured with a universal tensile tester (Zwick model 1445, Zwick GmbH & Co., Ulm, Germany) at a crosshead speed of 500 mm/min at room temperature. The average of three test values is reported for analysis.

Equilibrium swelling studies

The swelling behavior of the extrudate samples were measured by the sorption–desorption method. The molar percentage uptake of the solvents by the samples was measured at 25°C. The samples were cut to uniform dimensions of 20 mm of length and width and 2 mm of thickness. The initial weight of the samples was recorded before they were soaked in the solvent. The samples were immersed in different nonpolar (xylene, hexane, and diethyl ether) and polar (ethyl acetate, THF, and DMF) solvents. The swollen samples were weighed periodically with a time interval maintained after the removal of excess solvent from the surface by soft-wiping with filter paper. The molar percentage uptake of the solvent at time t (Q_t) was calculated from eq. (5):

$$Q_t = [(W_1 - W_0)/W_0]/M_w \times 100 \quad (5)$$

where W_0 and W_1 were the weights of the dry and swollen samples, respectively, and M_w is the molar mass of the solvent.

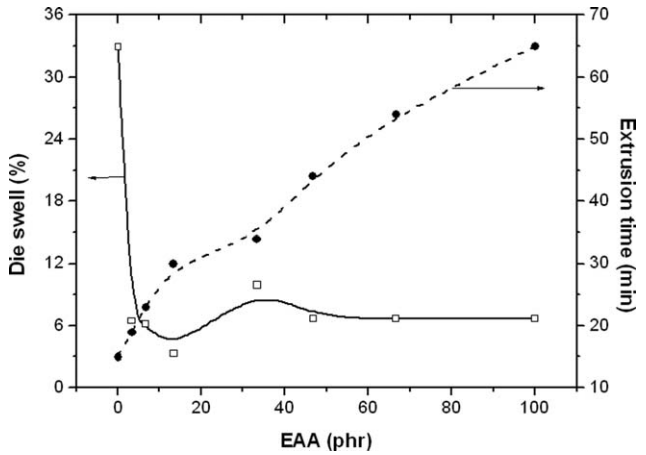

Figure 1 Plots of die swell (%) and extrusion time (min) versus different EAA concentrations.

RESULTS AND DISCUSSION

The specific gravity and the hardness values of all of the samples are reported in Table I. Pure POE had a hardness value of 36 (Shore D) according to the literature. We found the value to be 28 after it was crosslinked with 0.2 parts DCP; this was slightly lower than the reported value. This might have been due to a heat-softening effect of the mixing and molding operations on POE before hardness measurement. The rest of the compositions showed very close hardness values to both of the blend components POE and EAA; this indicated that the samples were still lighter and soft, even after modification with EAA and DCP at higher temperatures.

ΔGmix and χ

Theoretical predictions of ΔG_{mix} and χ for the POE–EAA system were made from the intercept (K) and slope (n), respectively, of the plot of $RT[(1/V_1)\varphi_1(\ln \varphi_1)] + [(1/V_2)\varphi_2(\ln \varphi_2)]$ versus $\varphi_1\varphi_2$. The value of ΔG_{mix} was obtained as -3.086 J/mol. The graphically determined ΔG_{mix} was the average free energy of mixing between POE and EAA over all of the compositions studied. A negative sign indicates gross thermodynamically favorable phase miscibility between POE and EAA, but its lower magnitude probably reveals the fact that mixing at all proportions might not have been favorable. χ was 57.94 for the POE–EAA blends; the moderately high χ value probably reflected good technical compatibility between the two polymer components.

Studies on the process parameters: Die swell and time of extrusion

Deformed polymer molecules under stress not only slide past each other but also tend to uncoil. On release of the deforming stresses, these molecules tend to revert to random coiled-up forms. Because molecular entanglements cause the molecules to act in a cooperative manner, some recovery of shape corresponding to the recoiling subject to elastic behavior takes place.[15] When leaving the die, the extended and oriented molecular chains of the molten polymer exhibit elastic recovery and return to their original random form, and the elastic energy is released because of the disappearance of an outside force field, and consequently, the diameter of the melt extrudate increases,[16] which is regarded as die swell. Figure 1 compares the die swell and extrusion time for different blend compositions. The die swell sharply decreased on addition of EAA to POE, probably because of a sharp reduction in the elastic behavior of the melt. Also, the addition of DCP may have crosslinked the polymer phase(s) under the process conditions and further reduced the die swell. Composition R_2 showed the maximum reduction; for other compositions and for neat EAA, the die swell was slightly higher than that of R_2 but was comprehensively lower than POE. The extrusion time (for 100 g of each batch) showed an almost steady increase from POE to neat EAA. This was ascribed to greater adhesion developed between the metal screw and EAA (polar material), which delayed the melt flow of the entire mass inside the barrel. *In situ* crosslinking of the polymer phase(s) may have also restricted the mass flow and increased the extrusion time.

FTIR spectroscopic analysis

Figure 2 shows normalized FTIR spectra of the representative POE–EAA systems after deconvolution of the peaks. The normalization was done with respect to the characteristic absorption peak at

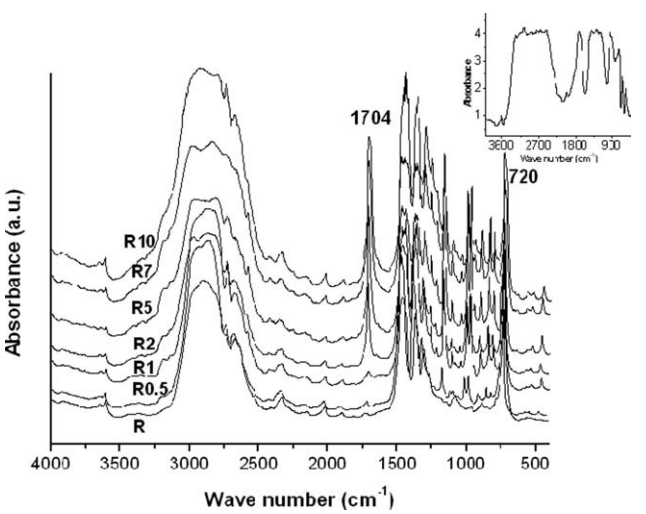

Figure 2 FTIR spectra of various samples; the spectrum for EAA is given in the inset.

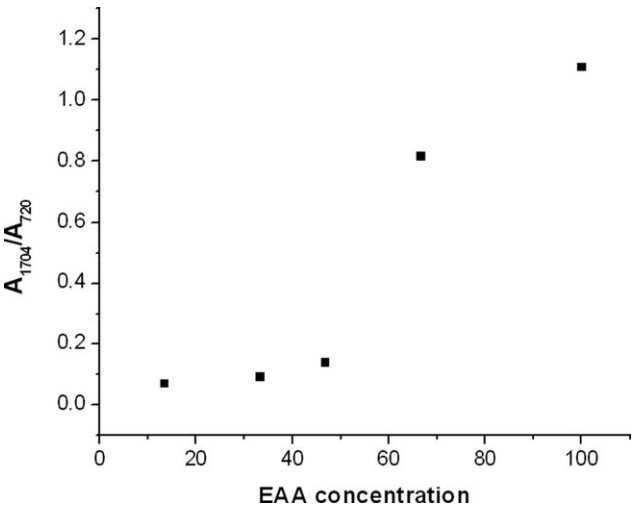

Figure 3 Plot of the ratio of the absorbance at 1704–720 cm^{-1} versus different EAA concentrations (phr). The error bars show the standard deviation.

720 cm^{-1} (the peak at 720 cm^{-1} results in hydrocarbon polymers only when pendant CH_2 unit exceeds 4 in number, for example, in the 1-octene comonomer side branch) of POE. The FTIR spectrum of neat EAA is shown in the inset for reference. Other characteristic absorption peaks of POE at 2840, 2928, and 1465 cm^{-1} were also observed for all of the samples. The addition of EAA generated a new peak at 1704 cm^{-1}; this corresponded to C=O stretching of AA in EAA. This was found to be present in all of the EAA-modified samples; its concentration gradually increased with increasing EAA proportions. This implied that EAA was arrested inside POE with DCP as a networking agent. A very small peak at 1704 cm^{-1} was also noticed for neat POE in Figure 2. This was probably due to the thermal oxidation of POE at the labile branch points as it underwent rigorous thermal treatments such as extrusions and moldings. The normalized peak ratio of 1704/720 was plotted against different EAA concentrations in Figure 3 to determine the relative compositions of POE and EAA in unknown samples, such as insoluble gels obtained after the solvent extraction of these blends.

Gel content analysis

The gel content analysis of all of these samples was measured from the mixed solvents of xylene (to extract the uncrosslinked POE phase) and DMF (to extract the uncrosslinked EAA phase) in a 50 : 50 wt % combination. The results are shown in Figure 4. The gel content of the blended samples increased steadily with increasing EAA content in the blends. The absorbance peak ratio, 1704/720 for the gels, plotted in Figure 4, showed the existence of EAA as the major phase (>90%) in the postextracted gel after the data points were compared with Figure 3 for known blend compositions. These results clearly indicate the formation of a semi-interpenetrating network (semi-IPN) type of blend structure because the major domain (POE) remained uncrosslinked and was extracted, whereas EAA was arrested as the major crosslinked phase inside the gel. DCP selectively crosslinked EAA but not POE under the prevailing process conditions, probably because of the greater steric resistance offered by longer octene branches in POE in comparison with pendant carboxylic acid moieties in EAA toward the chemical reaction of reactive macroradicals (free-radical formation took place more at the branch points than any other points on the macromolecules). The chemical structures of these macroradicals are shown in Scheme 1 for elucidation. This also showed that the principal reaction was between self-combining EAA macroradicals and only a few either cross-combinations between POE and EAA or self-combinations of POE radicals. The results were similar and in line with our earlier work on the grafting of AA onto octene and butene branched polyolefin elastomers, where the butene grade showed better grafting efficiency because of shorter branches.[9] The gel content analysis of the samples prepared with higher extrusion temperatures and DCP contents are further shown as the inset in Figure 4. The representative sample was R_2 because it exhibited the best processing properties so far. With increasing extrusion temperature with similar blend composition, the gel content increased, but the EAA content in the gel slightly decreased at the same time because the absorbance ratio gently fell below its original value obtained with R_2; similarly, with increasing DCP content at a fixed extrusion temperature of 200°C, there was a rise in the gel content

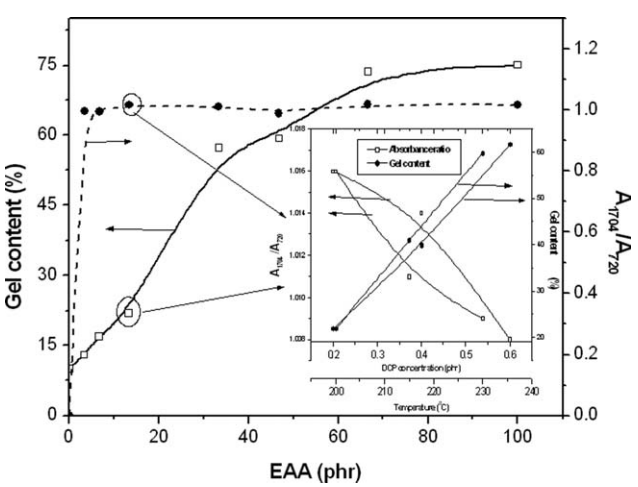

Figure 4 Plot of the percentage gel content versus different EAA concentrations (phr) added to POE. The effects of the change in gel content on various extrusion temperatures and DCP concentrations on sample R_2 is shown in the inset.

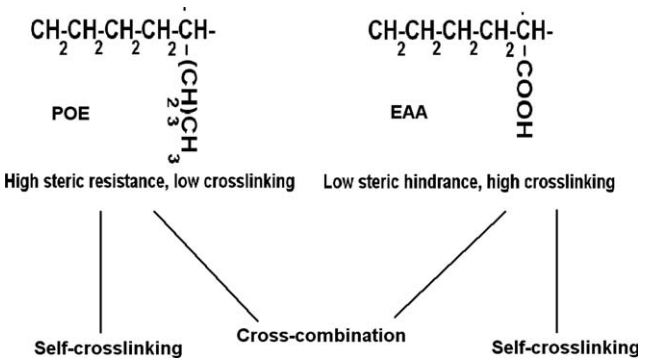

Scheme 1 Probable free radical sites on POE and EAA and their crosslink formation.

values and relative proportion of POE in the gel (see the downward trend in the peak absorbance ratio in Fig. 4). These showed that the blend morphology slightly changed as a higher DCP or temperature was applied for processing. More DCP generated more free radicals and increased the statistical probability for the reaction on both POE and EAA because some increased proportion of crosslinked POE was found to be present in the gel (the absorbance ratio decreased). Similarly, a higher extrusion temperature overcame the steric hindrance of the long pendant octene chains of POE (Scheme 1) and facilitated crosslinking on the same. The crosslinking of POE, although only slightly, under relatively drastic conditions (higher extrusion temperature and higher DCP concentration) may have been either homo (between POE macroradicals) or cross (between POE and EAA) types or may have been both, as stated earlier. Segregation between these structures could be made with solid-state NMR studies, but this was out of the scope of this study.

Measurement of θ and *W*

Figure 5 shows the variation in θ values with EAA addition; the results of *W*, just complementary to

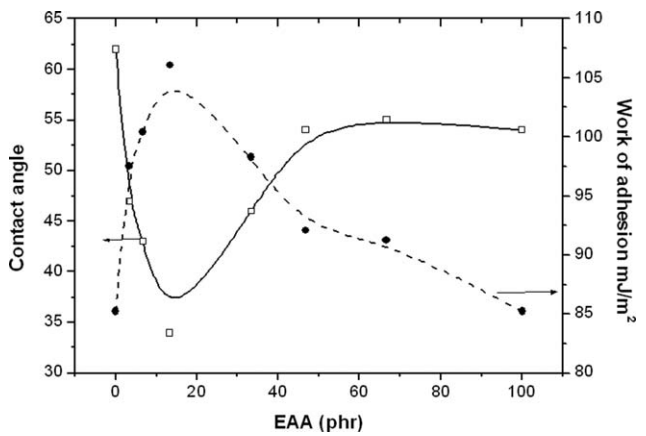

Figure 5 Plot of θ and *W* versus different EAA concentrations (phr) added to POE.

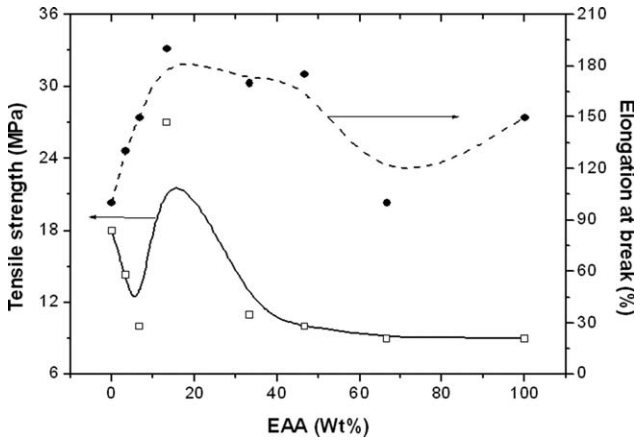

Figure 6 Plot of the tensile strength and elongation at break (%) as a function of EAA concentration (phr) added to POE.

θ data, calculated with eq. (4), are also plotted in the same figure. The sharp drop in θ values with the addition of EAA indicated a sharp rise in the polarity in POE. R_2 showed the minimum value; R_2's onward θ value increased for other samples. EAA showed a lower value than that of neat POE because of pendant COOH groups attached to main polyethylene chains. *W* showed the opposite trend, that is, a maximum for R_2 and lower values for other samples. To sample R_2, POE and EAA probably showed good phase mixing and, hence, developed excellent surface polarity. Beyond this composition, the phase compatibility may have become relatively weak (predicted earlier from ΔG_{mix} value) and affected the overall polarity of the hybrids. More of the single-phase crosslinked type morphology obtained with higher EAA contents (observed from the gel content analysis) probably also restricted interdiffusion of POE at higher EAA concentrations and resulted in improper phase mixing between these two. Also, EAA at higher concentrations probably developed poor technical compatibility with POE because of the greater surface energy differences.

Measurement of the mechanical properties: Tensile strength and elongation at break

The mechanical property analysis gave an idea about the bulk morphology of the hybrids. Figure 6 shows the variation in the tensile strength and elongation at break values at different EAA compositions. The tensile strength first decreased up to R_1, then increased and showed a maxima for R_2, and then finally decreased. The drop in tensile strength with the addition of EAA was due to a loss in the crystallinity of POE;[8] for R_2, the best interphase mixing (supported from other observations) and crosslinking of EAA showed synergism and exhibited comprehensively higher tensile strengths than those of neat POE. Other compositions, that is, R_2

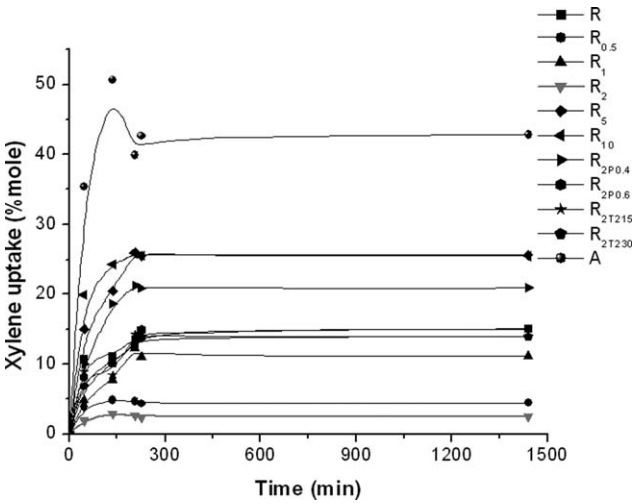

Figure 7 Plot of the nonpolar solvent (xylene) uptake (mol %) of various samples at different time intervals.

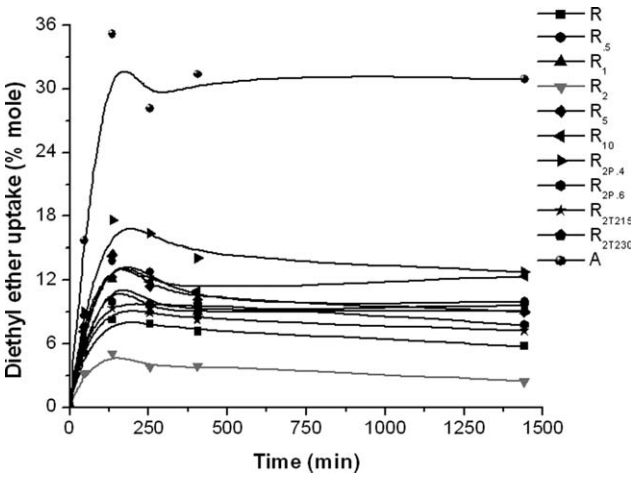

Figure 9 Plot of the nonpolar solvent (diethyl ether) uptake (mol %) of various samples at different time intervals.

onward, showed improper phase mixing between POE and EAA and, hence, exhibited lower tensile strengths. The elongation at break, on the other hand, increased with the addition of EAA because of a loss in the crystallinity of POE. For R_2 onward, this further decreased, probably because of phase separation in the hybrids; one phase got crosslinked, and its restricted flow accumulated stress inside the system and resulted in early failure.

Solvent resistance studies

Figures 7–12 show the solvent (nonpolar and polar) uptake characteristics of different POE–EAA semi-IPNs. The choice of solvents was based on their δ values, which were close to both the POE and EAA phases in the semi-IPN compositions. The nonpolar solvents were xylene, hexane, and diethyl ether. The results on the nonpolar solvent uptakes with time for different POE–EAA compositions along with those for neat POE and EAA are shown in Figures 7–9. In all cases, R_2 exhibited the lowest solvent uptake rate throughout the experiment; surprisingly, EAA showed a maximum solvent uptake rate. POE did not swell at an appreciable rate in these solvents at room temperature. The semi-IPNs prepared at higher DCP and higher temperatures were on par with other systems. The polyethylenic hydrocarbon part in EAA induced swelling in nonpolar solvents, despite being a polar polymer, whereas the substantial crystallinity of POE restricted its own swelling behavior. A drop in the crystallinity of POE due to the addition of EAA induced the fast diffusion of solvents inside the hybrids. R_2 was the best of all and contained entrapped POE in the evenly distributed and crosslinked EAA phase at the surface; this restricted the interdiffusion of nonpolar solvents inside the matrix.

The solvent uptake behavior in the three polar solvents, namely, ethyl acetate, DMF, and THF, are demonstrated in Figures 10–12. Ethyl acetate

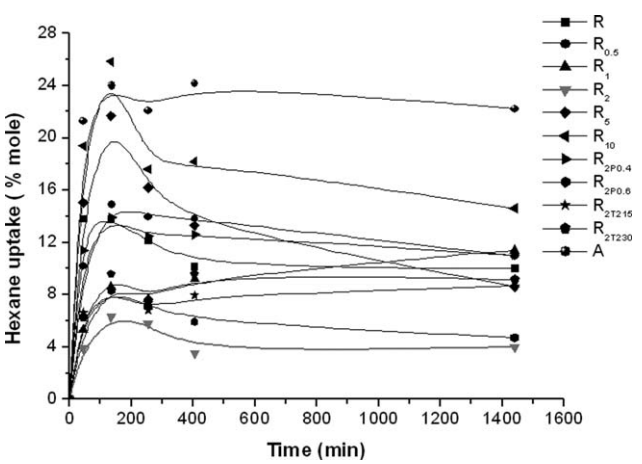

Figure 8 Plot of the nonpolar solvent (hexane) uptake (mol %) of various samples at different time intervals.

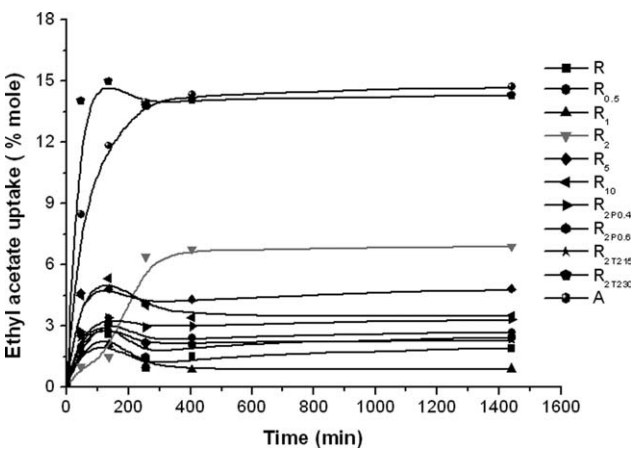

Figure 10 Plot of the polar solvent (ethyl acetate) uptake (mol %) of various samples at different time intervals.

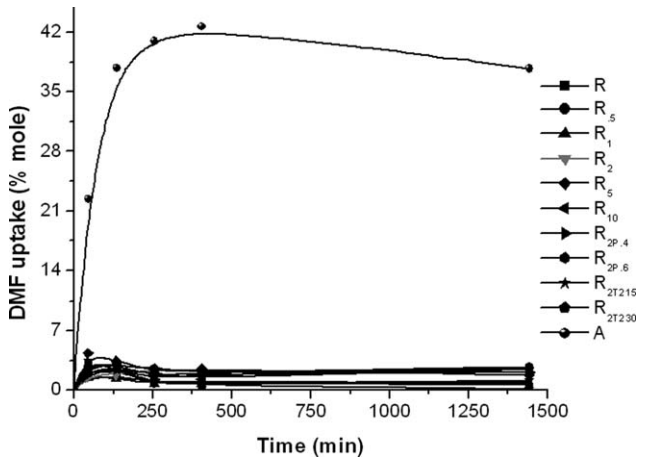

Figure 11 Plot of the polar solvent (DMF) uptake (mol %) of various samples at different time intervals.

diffused at a tremendous rate inside neat EAA and R_{2T230} and resulted in maximum swelling of these samples (Fig. 10). R_2, despite showing very high equilibrium swelling in ethyl acetate, exhibited the lowest swelling rate. R_1 showed minimum swelling behavior. EAA swelled tremendously in DMF and was virtually dissolved in it (Fig. 11). The rest of the samples demonstrated a significantly lower rate and were on par with R_2. In THF, almost no swelling of EAA took place (Fig. 12), and hence, the data points are not shown in the figure. Here, once again, R_2 demonstrated superior behavior as it showed maximum swelling resistance, both in terms of rate and state of swelling. The net solvent uptake of all of these networked blends against the δ values of different solvents are summarized in two diagrams for convenience, namely, Figure 13(a) for nonpolar solvents and Figure 13(b) for polar solvents. In nonpolar solvents, a mixed trend was observed, whereas the trend was quite similar in polar solvents. In the nonpolar category, there was an increase in the net solvent uptake, especially in hexane, as the net EAA

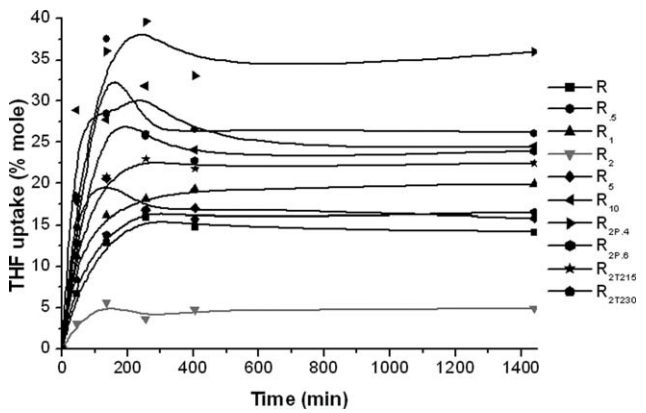

Figure 12 Plot of the polar solvent (THF) uptake (mol %) of various samples at different time intervals.

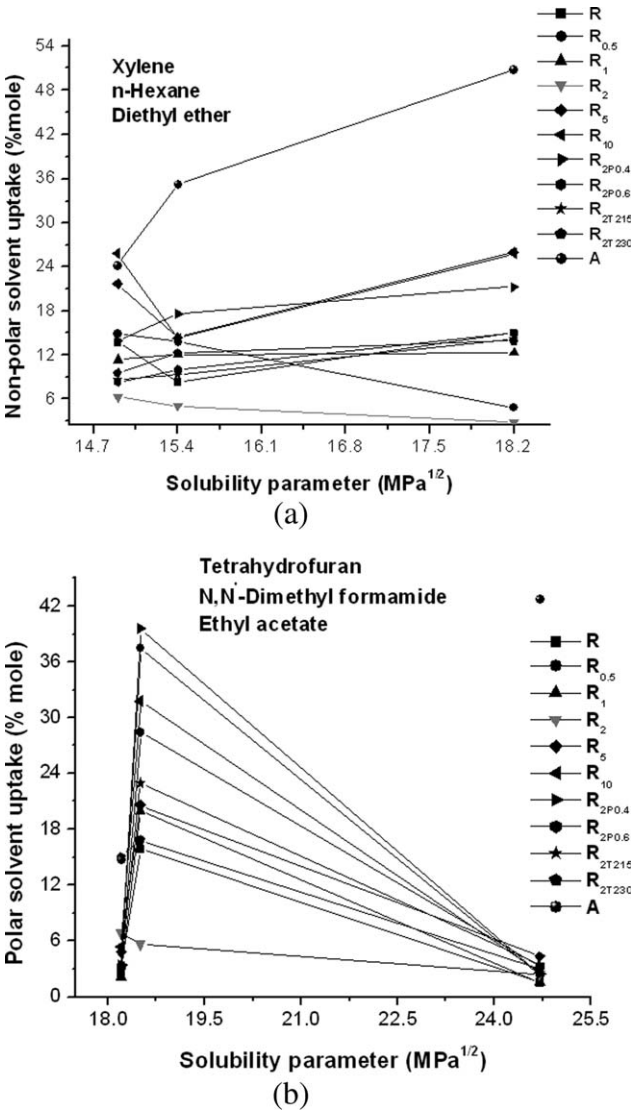

Figure 13 Plot of the net solvent uptake by different blends against δ values of the solvents: (a) nonpolar and (b) polar solvents.

content increased. This was understandable, as neat EAA showed the highest swelling behavior in these solvents. The exception was R_2; it demonstrated the lowest swelling behavior, as already mentioned. An increase in the peroxide dose certainly reduced the net swelling behavior of the samples, such as $R_{2P0.4}$ and $R_{2P0.6}$, but an increase in the extrusion temperature showed reverse characteristics [R_{2T215} and R_{2T230} in Fig. 13(a)]. The net solvent uptake behavior in polar solvents, plotted in Figure 13(b), showed minimum swelling in ethyl acetate and DMF (neat EAA swelled tremendously in DMF) and maximum swelling in THF for all of the samples. R_2 in this series was not the best composition, as showed the highest solvent uptake in ethyl acetate (other than R_{2T230} and A) and a only slightly higher uptake in DMF than some of the blend compositions, as

TABLE II
***n* and K Values of R_2 in Different Solvents**

Solvent	δ (δ; $MPa^{1/2}$)	*n*	$K \times 10^2$ (g/g min)
Xylene (nonpolar)	18.2	0.373	1.0476
Hexane (nonpolar)	14.9	0.276	1.0111
Diethyl ether (nonpolar)	15.4	0.310	1.2017
Ethyl acetate (polar)	18.2	0.303	0.9951
DMF (polar)	24.7	0.185	1.0116
THF (polar)	18.5	0.529	1.0332
POE	16.68		
EAA	18.3		

shown in Figure 13(b). This was probably due to the closeness in the δ data of EAA and ethyl acetate (recorded in Table II) developing compatibility with the hybrid and the solvent. In DMF, in fact, all of the network blends exhibited very good resistance toward swelling, maybe because of the very high solvent polarity. Solvent uptake modeling of all kinds of blends demonstrated the best overall performance by sample R_2, which was composed of 13.3 wt % EAA and 0.2 wt % DCP and was extruded at 200°C. Because of this, we carried out further kinetic investigation on the solvent swelling behavior of this semi-IPN sample with eq. (6), considering the transport mechanism:

$$M_t/M_\infty = Kt^n \tag{6}$$

where M_t and M_∞ are the weight percentage uptakes of the solvent at time t and at the equilibrium swelling states, respectively,[15] and n and K are kinetic parameters.

The logarithmic form of eq. (6) is represented by eq. (7):

$$\log(M_t/M_\infty) = \log K + n(\log t) \tag{7}$$

The kinetic parameters were determined from n and K of the log–log plot of M_t/M_∞ versus t (not shown in this article) and are reported in Table II. K depended on the structural aspects of the blend and its interaction with the solvent, whereas n implied the mode of solvent diffusion. The range of interaction with different solvents did not vary, even when solvents of different δ's were used. This was probably due to the coexistence of both polar and nonpolar phases in R_2. The value of n never crossed the 0.5 mark, except for THF. This indicated that the solvent intake was primarily via Fickian diffusion, but in THF, it depended on the molecular relaxation of the network hybrid.

CONCLUSIONS

Polar modification of POE was achieved by the use of a newer approach in this investigation. POE was coextruded with EAA with DCP as a crosslinker under melting. The EAA concentration varied from 0 to 100 wt % and gave a net polarity of 0–15 wt %. The combination of POE and EAA showed a slightly negative thermodynamic compatibility, as predicted from theoretical calculations. All of the resulting hybrids were lighter and also possessed similar softnesses as those of the base elastomer. The gel content analysis showed that extrusion of the samples at 200°C with 0.2 wt % DCP generated semi-IPNs, where the POE was arrested inside the crosslinked EAA phase; this morphology changed slightly with increasing DCP and extrusion temperatures because some crosslinked POE was identified along with EAA in the postextracted gels. The sample containing 13 wt % EAA and 0.2 wt % DCP was assigned as the best composition, as it gave superior surface polarity and mechanical properties and excellent resistance toward room-temperature swelling inside both the polar and nonpolar solvents compared to neat POE and EAA. The excellent phase mixing and uniform distribution of the crosslinked EAA phase inside POE matrix generated strong diffusion resistance against different solvents compared to all of the other compositions.

References

1. de Souza, R. F.; Casagrande, O. L. Macromol Rapid Commun 2001, 22, 1301.
2. Da Silva, A. L.; Tavares, M. I.; Politano, D. P.; Coutinho, F. M. B.; Rocha, M. C. G. J Appl Polym Sci 1977, 66, 2005.
3. Engage Product Data Sheet. http://www.dow.com (accessed June 2007).
4. Hwang, Y. C.; Chum, S.; Sehanobish, K. Annu Tech Conf 1994, 94, 3414.
5. McNally, T.; McShane, P.; Nally, G. M.; Murphy, W. R.; Cook, M.; Miller, A. Polymer 2002, 43, 3785.
6. Zhu, L.; Xu, X.; Wang, F.; Song, N.; Sheng, J. Mater Sci Eng A 2008, 494, 449.
7. Yu, Z. Z.; Ke, Y. C.; Ou, Y. C.; Hu, G. H. J Appl Polym Sci 2000, 76, 1285.
8. Yu, Z. Z.; Ou, Y. C.; Qi, Z. N.; Hu, G. H. J Polym Sci Part B: Polym Phys 1998, 36, 1987.
9. Biswas, A.; Bandyopadhyay, A.; Singha, N. K.; Bhowmick, A. K. J Appl Polym Sci 2007, 105, 3409.
10. Biswas, A.; Bandyopadhyay, A.; Singha, N. K.; Bhowmick, A. K. J Polym Sci Part A: Polym Chem 2007, 45, 5529.
11. Wu, C. S.; Lai, S. M.; Liao, H. T. J Appl Polym Sci 2002, 85, 2905.
12. González, I.; Eguiazábal, J. I.; Nazábal, J. Polym Test 2009, 28 760.
13. Arostegui, A.; Nazabal, J. Polymer 2003, 44, 239.
14. Arostegui, A.; Gaztelumendi, M.; Nazabal, J. Polymer 2001, 42, 9565.
15. Jiao, C.; Wang, Z.; Gui, Z.; Hu, Y. Eur Polym J 2005, 41, 1204.
16. He, P.; Huang, H.; Zhang, Y.; Liu, N. C. React Funct Polym 2005, 62, 25.